

Neutrino oscillations: the rise of the PMNS paradigm

Claudio Giganti

*LPNHE, CNRS/IN2P3, Université Pierre et Marie Curie, Université Paris Diderot,
Paris 75252, France*

Stéphane Lavignac

IPhT, CEA Saclay, 91191 Gif-sur-Yvette CEDEX, France

Marco Zito

IRFU/SPP, CEA Saclay, 91191 Gif-sur-Yvette CEDEX, France

Abstract

This is the abstract

Keywords:

1. Introduction

Introduction

2. Theory and phenomenology of oscillations 15 pg SL

2.1. Preliminary

Lagrangian NC and CC, ν in SM, m ?

2.2. Basis

U PMNS : D vs M, oscillation independent of D/M vacuum N=2 N=3

2.3. matter

$n=\text{const} \rightarrow$ MH determination

2.4. MSW

adiabatic regime

2.5. CP violation

CP violation vacuum (+ CP with matter ?)

3. Oscillation parameters: current status 30pg

3.1. The solar sector: SK, SNO, KamLAND (SL)

reactions + spectrum nu solar (plot)

Davis first indication deficit Ga/Sage confirmation, E dependence

SK measure spectrum vs E plot

SNO measure NC/CC \rightarrow Φ (nu other)/ Φ (nue) plot

Kamland confirmation artificial beam (vacuum) E/L oscillation plot precision meas. $\Delta m^2 \rightarrow$ excludes LOW \rightarrow LMA

(MSW interpretation) Borexino measure various components of the spectrum (Be, CNO) \rightarrow confirmation MSW (upturn) day night effect
ref

3.2. The atmospheric sector (MZ)

In this subsection we will describe the status of the so called atmospheric neutrino oscillations, i.e. the 3-2 oscillations that were first discovered in the study of atmospheric neutrinos and later were precisely measured with the use of long baseline neutrino beams.

3.2.1. The atmospheric neutrino flux

The atmosphere is constantly bombarded by primary cosmic rays, composed mainly of protons, with a smaller component of α particles and heavier nuclei. The interaction of these particles with atomic nuclei in the atmosphere produces hadronic showers composed mainly of pions and kaons. The decay of these mesons according to $\pi^+ \rightarrow \mu^+ \nu_\mu$ followed by $\mu^+ \rightarrow e^+ \nu_e \bar{\nu}_\mu$, $K^+ \rightarrow \pi^+ \nu_\mu$ and $K_L \rightarrow \pi^+ e^- \nu_e$ together with their charge conjugated processes, produces a flux of ν_μ and ν_e with a steeply falling power-law spectrum (Fig. 1).

The calculation of this neutrino flux [?] relies on the knowledge of the primary flux and composition, of the Earth magnetic field, and of the hadro-production cross-section. Recent studies [? ? ?] taking into account 3D effects and recent measurements of the hadro-production cross-sections largely improve on previous efforts and reach precisions of 7-8 % for the flux in the 1-10 GeV range. It should be noticed that the ratio $N(\nu_\mu + \bar{\nu}_\mu)/N(\nu_e + \bar{\nu}_e)$ is predicted with a much better precision of a few % as several systematic

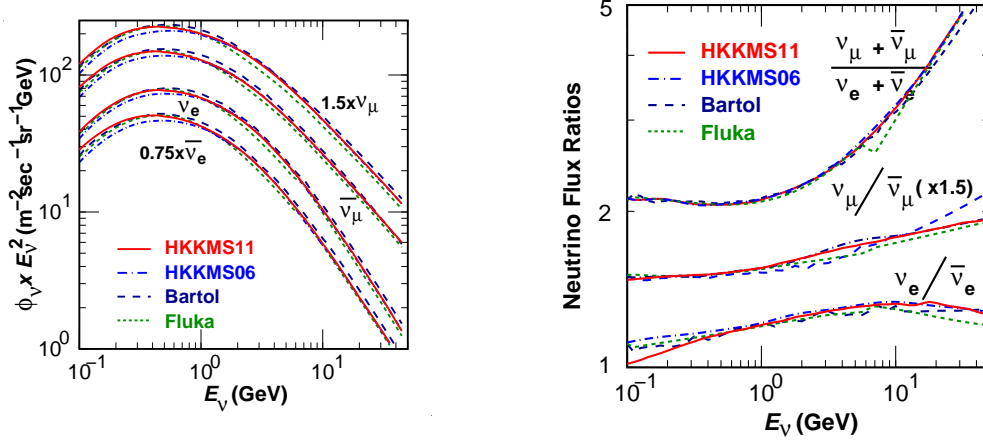


Figure 1: The flux of atmospheric neutrinos (left) and several flux ratios (right) [?].

uncertainties cancel in this ratio. In the limiting case where all the muons from pion decays decay themselves in flight, this ratio is close to 2, as can be easily deduced from the decay processes mentioned above.

3.2.2. The early days, the up-down asymmetry and controversy

The study of atmospheric neutrinos started in the 1960: two experiments in very deep mines, in South Africa [?] and in India [?], observed muons produced by their interactions. In the 1980, several massive underground experiments, mainly motivated by the search for the proton decay predicted by Grand Unification theories, started collecting data. These experiments needed to study in detail atmospheric neutrino interactions as they constitute a background for proton decay searches.

In 1988, Kamiokande reported a deficit in the number of ν_μ of events, while the number of ν_e events agreed with the prediction. This started the so-called atmospheric neutrino anomaly. This deficit was also observed by the IMB experiment and later by MACRO and SOUDAN-2, while Fréjus and NUSEX observed no deficit.

3.2.3. The evidence for atmospheric neutrino disappearance

The situation evolved rapidly with the advent of Super-Kamiokande, that started data-taking in 1996. Super-Kamiokande is very large water Cherenkov detector located in the Mozumi mine (Gifu prefecture, Japan), under a 1000 m rock overburden, equivalent to 2700 m of water. It is a stainless steel tank (41.4 m high, 39.3 m diameter) containing 50 kt of ultra-pure

water. The detection volume is partitioned in an outer detector, composed of 1885 8 inch PMTs, and an inner detector with 11146 20 inch PMTs. The fiducial volume is 22.5 kt. Super-Kamiokande could rapidly accumulate a rather large data set of atmospheric neutrinos, measuring the direction of the produced lepton, its energy for fully contained events and their nature. Above a few hundred MeV/c, the direction of the produced lepton is strongly correlated to the direction of the incoming neutrino.

In 1998, the Super-Kamiokande collaboration presented their first analysis of atmospheric neutrinos [?], in particular the distributions of zenith angle for ν_μ and ν_e event selections (see Fig. 2 for an updated distribution) based on 33 kton year. This was the first compelling evidence for neutrino oscillations as the explanation of the previously mentioned anomaly.

Indeed the neutrino path from the production to the detection varies from 15 km for down-going neutrinos (cosine of the zenith angle equal to 1) to more than 12000 km for up-going neutrinos having traversed the whole Earth (cosine of the zenith angle equal to -1), thereby probing a large span of possible oscillation lengths.

In a two neutrino scenario, the ν_μ disappearance is governed by $\sin^2(2\theta) \sin^2(4\Delta m^2 L/E)$, where θ is the relevant mixing angle and Δm^2 the squared-mass difference of the mass eigenstates. A glance at Fig.2 reveals several important overall features:

- there is a strong disappearance of ν_μ , especially visible for up-going neutrinos. As the survival probability for very long baseline approaches $1/2 \sin^2(2\theta)$, and the observed survival probability is close to 0.5, the mixing angle is therefore close to the maximal value $\pi/4$.
- The disappearance sets in for neutrinos close to horizontal zenith angle, and therefore the oscillation length should be of the order of 400 km for energy around 1 GeV, or $\Delta m^2 \simeq 10^{-3} \text{eV}^2$.
- There is no sizeable excess or deficit of ν_e . Therefore the oscillations of ν_μ should mainly involve either $\nu_\mu \rightarrow \nu_\tau$ or $\nu_\mu \rightarrow \nu_s$, where ν_s is an additional neutrino state.

Independently of any accurate predictions of the neutrino flux, the experimental observation of the distributions of Fig.2 is sufficient to make a strong case for neutrino disappearance. Indeed, above several GeV, the neutrino flux is isotropic, as the primary cosmic rays are not deflected in a significant

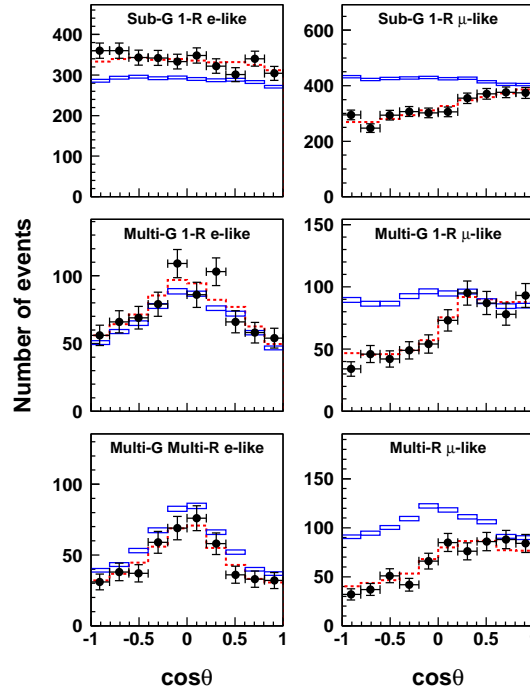


Figure 2: Zenith angle distributions of Super-Kamiokande atmospheric neutrino events from [?]. Fully contained e-like, μ -like events are shown for data (filled circles with statistical error bars), MC distributions without oscillation (boxes) and best-fit distributions (dashed). The box height shows the statistical error.

way by the geomagnetic field. The observation of a zenith angle dependent deficit of the neutrinos is then a sufficient argument to conclude that these neutrinos undergo a non-standard propagation.

While in 1998 other hypotheses like decay or decoherence were still open, more recent data from long baseline accelerator experiments have ruled out all explanations apart from oscillations because the alternative hypotheses imply a different L/E behaviour.

The IceCube experiment at the South Pole has recently completed the installation of DeepCore, a denser array of optical modules, aimed at significantly lowering the muon threshold. With data recorded between 2011 and 2014, corresponding to 5074 observed events, they have recently published an analysis of the disappearance of atmospheric ν_μ [?] in the range 10-100 GeV, requiring the zenithal angle to satisfy $\cos\theta < 0$, which has a similar sensitivity to that of Super-Kamiokande (Fig. 3) with the prospects of further improvements.

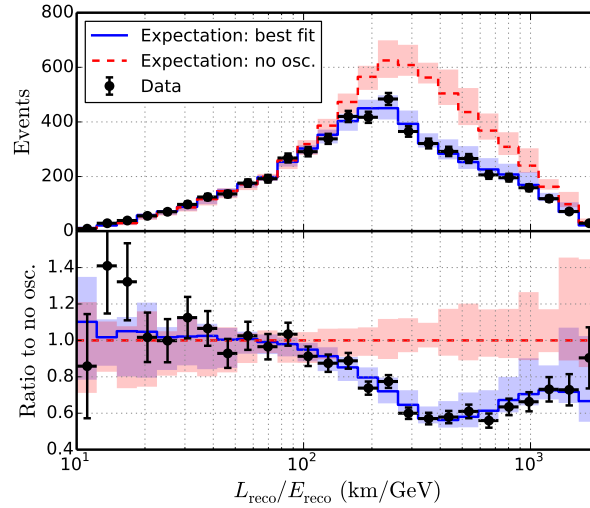


Figure 3: Distribution of atmospheric neutrino events measured by the IceCube experiment[?] as a function of reconstructed L/E. Data are compared to the best fit and expectation with no oscillations (top), and the ratio of data and best fit to the expectation without oscillations is also shown (bottom). Bands indicate estimated systematic uncertainties.

3.3. Long-baseline neutrino beams

Neutrino beams [?] based on particle accelerators have been used since the 1960s, when they provided the evidence for the existence of two types of neutrino, ν_e and ν_μ . The general design is based on a high intensity proton beam impinging on a target and producing pions and kaons through interactions on the target nuclei. These mesons decay in a dedicated volume downstream of the target, creating mainly a ν_μ beam.

The long baseline beams are based on the so called wide band beam concept. Here the secondary charged mesons are focused using a system of magnetic devices, called horns. The horns, usually with a cylindrical symmetry around the beam, are pulsed with a very intense current in coincidence with the arrival of the beam.

The flux is tuned in such a way that the phase $\Delta m_{32}^2 L / (4E)$ reaches $\pi/2$ for the design baseline L and the peak energy E , in order to probe the atmospheric oscillation sector with the beam ν_μ . To do so, the proton energy, the target length and width, the focussing system and the decay volume length and width need to be accurately designed and optimized.

An off-axis neutrino beam [?] relies on the following idea: as the ν_μ are mainly produced by the two-body decays of pions, there is a correlation between pion energy E_π , the neutrino energy E_ν and the decay angle θ

$$E_\nu = \frac{(1 - (m_\mu/m_\pi)^2)E_\pi}{(1 + \gamma^2\theta^2)} \quad (1)$$

valid in the limit of small angles.

Neutrinos emitted at a small angle with respect to the pion direction have a distinct narrow spectrum peaking at a much lower energy with respect to the on axis beam. This feature that has been used by the T2K and NO ν A experiments, offers several advantages because it avoids the large high energy tail of the on axis beam, thereby reducing some background reactions.

As the neutrino beam is a tertiary beam, it is necessary to include in the experimental apparatus monitoring devices to ensure that it is stable in intensity and direction. To this effect, muon detectors, sensitive to the muons produced by the pion decays, are placed close to the end of the decay volume. Moreover, as the neutrino flux and cross-sections and the beam composition are not known with sufficient precision, a near detector is located close to the target station (typically within a few hundred meters). The near detector constrains the neutrino interaction rate, proportional to the product $t \times \text{of}$

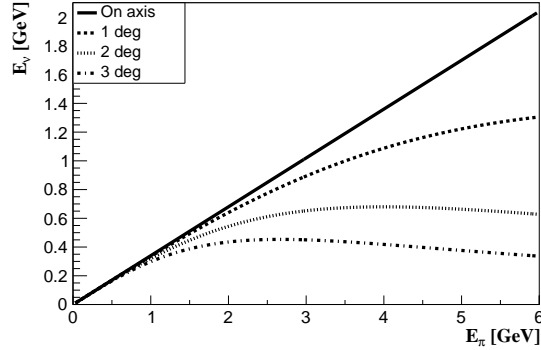


Figure 4: Neutrino energy as a function of the pion energy for on-axis decays and several off-axis angles. For a non-zero off-axis angle, the neutrino energy reaches a maximum. This feature is currently exploited in the T2K and NO ν A experiments.

Exp.	Energy (GeV)	Power (kW)	L (km)	FD mass (kt)	POT
K2K	30		250	22.5	1.8 10^{20} 8 10^{21}
MINOS	120	700	790	5.4	
OPERA	450	732			
T2K	30	750	295	22.5	
NO ν A	120	700	810	14	
HK	30				
DUNE	120	1200	1300	40	

Table 1: Parameters of recent and future long baseline experiments. Energy and power refer to the primary proton beam, L is the baseline, FD the mass of the far detector. POT (Proton On Target) represents the integrated dataset as of 2016.

neutrino flux and the cross-section. Moreover, the near detector allows to measure the beam composition and to perform study of several neutrino cross-section.

Description of T2K beam line if space allows.

3.3.1. Flux and cross-section systematic uncertainties in long-baseline experiments

The measurement of neutrino oscillations has now entered the precision era. Particularly long-baseline neutrino oscillation experiments require a deep knowledge of the systematic uncertainties related to neutrino fluxes and neutrino cross-sections to perform measurements of oscillation parameters.

A common strategy to reduce systematic uncertainties, used in most of the long baseline experiments, is the use of a Near Detector complex, located at few hundreds of meters from the beam target where neutrinos are detected before the oscillations. In this way the neutrino spectrum and the flavor composition of the beam can be precisely measured before the oscillations and is used to determine the expected spectra at the far detector if there were no oscillations.

Some long-baseline experiments, as for example MINOS and NO ν A, uses as near detector a detector that has the same composition as the far detector so that cross-section uncertainties due to the different target nuclei or detector systematic uncertainties are minimized in the extrapolation. Other experiments, as for example K2K and T2K, uses a set of near detector, with different target nuclei, in order to maximize the information on the cross-section models.

In this section, as an example, we will briefly describe how the T2K experiment uses the near detector data to reduce the systematic uncertainties in the oscillation analysis. The T2K near detector, called ND280, is magnetized, with several sub-detectors installed within the ex UA1/NOMAD magnet that provides a 0.2 T magnetic field. For the oscillation analysis the ND280 tracker system is used, comprising 2 Fine Grained Detectors (FGD) interleaved to 3 Time Projection Chambers (TPC). The FGDs act as an active target for neutrino interactions (each with a mass of ~ 1.5 ton (check)). Particles produced in the FGD enter the TPCs where the charge and the momentum of the tracks is reconstructed as well as the particle identification based on the measurement of the energy loss in the gas.

At T2K energies most of the ν_μ charged current neutrino interactions produce only one track in the final state, the muon. In some cases the neutrino gives enough energy to the target nuclei producing also pions or protons that can also enter the TPC. The presence of the magnetic field allows to reconstruct the charge of the muon, distinguishing between negative muons produced by ν_μ and positive leptons produced by $\bar{\nu}_\mu$ interactions.

3.3.2. Results from long-baseline accelerator experiments K2K MINOS T2K NO ν A

K2K (KEK-to-Kamioka) was the first long baseline neutrino beam, using Super-Kamiokande as its far detector at 290 km from the neutrino production. Operating between 1999 and 2004, it has measured the disappearance of ν_μ : 112 events were observed, while $158.1^{+9.2}_{-8.6}$ were expected without oscilla-

tion, a 4.3σ effect [?]. This measurement has confirmed neutrino oscillation as the explanation for the atmospheric neutrino disappearance.

Further precision measurements of the $\nu_\mu \rightarrow \nu_\mu$ were reported by MINOS, T2K and NO ν A. In particular, T2K and NO ν A use a narrow band beam, based on the off-axis design, that is particularly suited for the measurement of ν_μ disappearance once the mass square difference is known. For a given Δm_{32}^2 and a given baseline distance, in fact, the oscillation probability depends on the neutrino energy that can be tuned by changing the off-axis angle. In the case of T2K (L=295 km) the maximum of the oscillation is at an energy of 600 MeV while in the case of NO ν A (L=810 km) the maximum is at 1800 MeV.

While the most recent analyses published by T2K do a global fits of appearance and disappearance modes to extract the maximum of the information on neutrino oscillations in the PMNS framework, disappearance analyses only have also been done by T2K in order to test the PMNS framework. In the ν_μ disappearance probability in fact there are no CP odd terms so the disappearance probability is expected to be the same for ν_μ and $\bar{\nu}_\mu$. Previous results from MINOS showed some tensions between neutrinos and antineutrinos. Based on 7.482×10^{20} protons-on-target (POT) collected in neutrino mode and 7.471×10^{20} POT collected in antineutrino mode, T2K has observed 135 (66) ν_μ ($\bar{\nu}_\mu$) candidates at SK with 522 (185) events expected in case of no-oscillations and 135.8 (64.2) events expected for maximum disappearance. The reconstructed energy spectrum for both, ν_μ and $\bar{\nu}_\mu$ surviving events are shown in Fig. ???. Thanks to the use of the Near Detector data described in Sect. 3.3.1, the systematic uncertainties on these measurements are smaller than 5% and a precise measurement of θ_{23} and Δm_{32}^2 is obtained as shown in Fig. ??. The oscillation parameters measured are in excellent agreement between neutrinos and antineutrinos and both are compatible with maximal mixing for θ_{23} .

NO ν A has also reported a measurement of ν_μ disappearance using 6.05×10^{20} POT and by selecting μ -like candidates at the far detector. They observed 78 events in the far detector, while 473 ± 30 were expected without oscillations. This result lead to some tensions, especially with the T2K experiment, since maximal mixing is excluded by NO ν A at 2.5σ as shown in Fig. ??.

The two collaborations are working to understand this difference that could still be simply due to statistical fluctuations. A comparison between reconstructed energy spectrum for the best-fit and the one obtained by imposing maximal mixing in NO ν A is shown in Fig. ??. Something similar

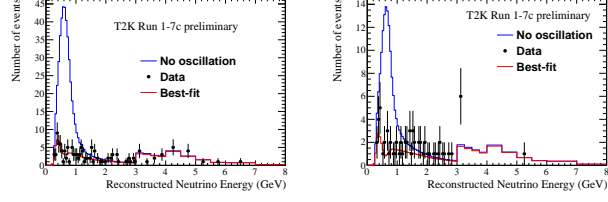


Figure 5: Reconstructed ν_μ and $\bar{\nu}_\mu$ energy spectrum by the T2K collaboration for data, best-fit prediction, and unoscillated prediction.

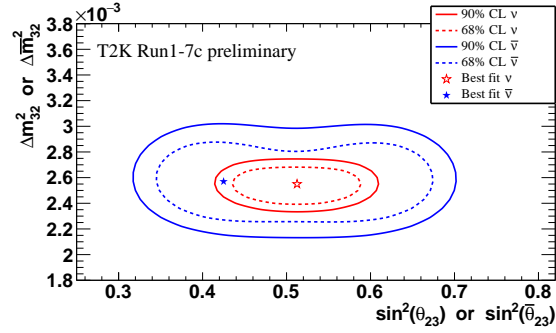


Figure 6: Δm^2 versus $\sin^2(\theta_{23})$ for neutrinos and antineutrinos parameters. The constant $\Delta\chi^2$ critical values in the gaussian approximation are shown.

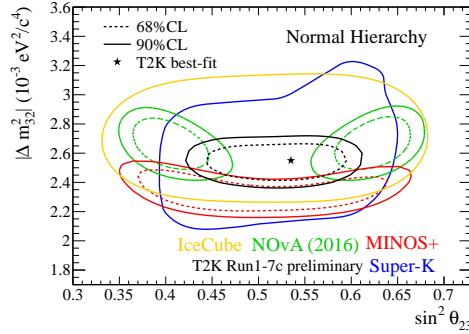


Figure 7: Measured $\Delta\chi^2$ distributions as a function of $\sin^2 \theta_{23}$, $\Delta m_{32}^2(\Delta m_{13}^2)$ for T2K, Super-K (PoS ICRC2015 (2015) 1062), Minos+ (Neutrino 2014 conference), NOvA (Phys.Rev. D93 (2016) 051104, arXiv 1601.05037) and IceCube DeepCore (Phys.Rev. D91 (2015) 072004, arXiv 1410.7227).

is done by T2K comparing their data, the T2K best fit and the spectrum obtained by imposing the NOvA best-fit oscillation parameters as shown in Fig. ?? . Additional data from both, T2K and NOvA will help to clarify the situation.

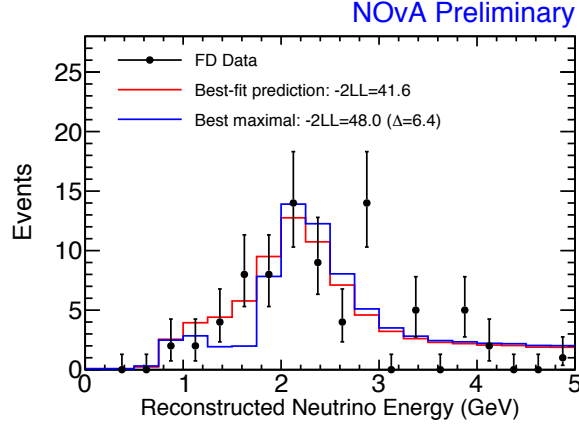


Figure 8: Reconstructed energy spectrum in NOvA for data, best fit and best fit assuming maximum mixing

3.3.3. Evidence for ν_τ appearance

The OPERA experiment on the CERN to Gran Sasso neutrino beam, taking data between 2008 and 2012, was designed to test the $\nu_\mu \rightarrow \nu_\tau$ appearance hypothesis. The detector is based on the Emulsion Cloud Chamber technique, with 1800 ton of nuclear emulsion detectors in the forms of bricks, each brick being composed of a stack of nuclear emulsion film and lead plates. This target, capable of sub-micrometric track resolution, is devoted to the study of the neutrino interaction vertex and the particles associated to it. The identification of the τ leptons relies mainly on their characteristic kink (Fig. ??) due to the decay $\tau \rightarrow h\nu_\tau$, or $\tau \rightarrow l\nu_\tau\bar{\nu}_l$, where h is a charged meson, and l is an electron or a muon. Another signature is related to the decay $\tau \rightarrow 3h\nu_\tau$ where the short τ track ends in a three-pronged vertex. The target detectors are complemented by scintillator trackers and muon spectrometers.

OPERA has observed 5 ν_τ candidate events [?] with a total background of 0.25 ± 0.05 events, mainly coming from decays of charmed particles. This corresponds to a 5.1σ observation of ν_τ production in an oscillated ν_μ beam.

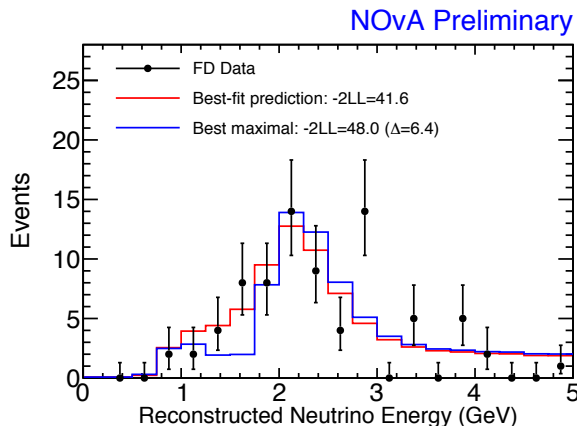


Figure 9: Reconstructed energy spectrum in NO ν A for data, best fit and best fit assuming maximum mixing

The Super-Kamiokande collaboration has also searched for ν_τ appearance in multi-ring events to test the hypothesis of $\nu_\mu \rightarrow \nu_\tau$ oscillations [?]. While the selected sample is affected by large backgrounds, there is an excess of tau-like events in the upward-going direction with a significance of 3.8σ , offering a complementary confirmation of the OPERA result.

3.4. The 1-3 sector (MZ)

Solar and atmospheric results are well described by two-flavour mixing models, but we know that there are at least three neutrino flavours and therefore at least three mass eigenstates. The experiments described so-far, while giving robust evidence for neutrino oscillation, do not provide a full picture of 3x3 mixing models.

In order to fully establish the PMNS matrix it is necessary to measure the last mixing angle, θ_{13} . A non-zero value of θ_{13} is required to have CP violation in the lepton sector. The parameter θ_{13} can be measured by reactor neutrino experiments through the measurement of $\bar{\nu}_e$ disappearance at short baselines ($\sim 1 \text{ km}$) or by long-baseline accelerator experiments by looking for electron neutrino appearance in the ν_μ beam. Reactor experiments directly measure θ_{13} by observing $\bar{\nu}_e$ disappearance according to the simple equation:

$$P(\bar{\nu}_e \rightarrow \bar{\nu}_e) = 1 - \sin^2 2\theta_{13} \sin^2(1.267\Delta m_{13}^2 L/E) \quad (2)$$

This is not the case in long-baseline accelerator experiments for which the

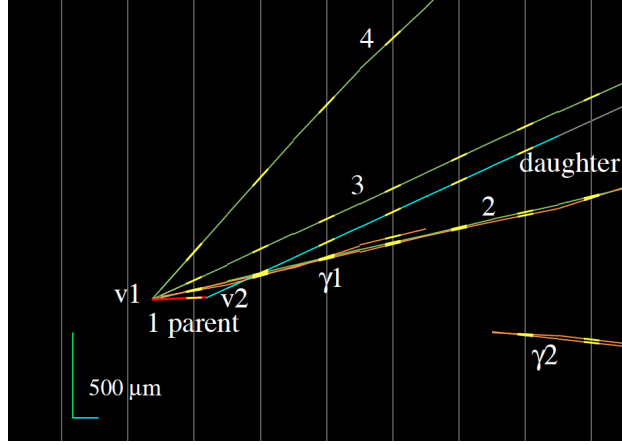


Figure 10: Event display of the fourth ν_τ candidate event from the OPERA experiment [?] in the horizontal projection longitudinal to the neutrino direction. The primary and secondary vertices are indicated as V_0 and V_1 , respectively. The kink between the parent and daughter track, a feature of τ lepton decays, is clearly visible. The yellow stubs represent the track segments as measured in the emulsion films.

ν_e appearance probability is a sub-leading effect of the oscillation involving Δm_{32}^2 in which ν_μ mainly oscillate into ν_τ . The general expression for $P(\nu_\mu \rightarrow \nu_e)$ is a complicated formula that can be derived considering the formalism for the three neutrino families and depends on a combination of θ_{13} , δ_{CP} and matter effects due to the large amount of matter crossed by neutrinos before reaching the detector. An approximated expression of this probability is:

$$\begin{aligned}
P(\nu_\mu \rightarrow \nu_e) = & 4C_{13}^2 S_{13}^2 S_{23}^2 \sin^2 \phi_{31} \\
& + 8C_{13}^2 S_{12} S_{13} S_{23} (C_{12} C_{23} \cos \delta_{CP} - S_{12} S_{13} S_{23}) \cos \phi_{32} \sin \phi_{31} \sin \phi_{21} \\
& - 8C_{13}^2 C_{12} C_{23} S_{12} S_{13} S_{23} \sin \delta_{CP} \sin \phi_{32} \sin \phi_{31} \sin \phi_{21} \\
& + 4S_{12}^2 C_{13}^2 (C_{12}^2 C_{23}^2 + S_{12}^2 S_{23}^2 S_{13}^2 - 2C_{12} C_{23} S_{12} S_{23} S_{13} \cos \delta_{CP}) \sin^2 \phi_{21} \\
& - 8C_{13}^2 S_{13}^2 S_{23}^2 \frac{aL}{4E_\nu} (1 - 2S_{13}^2) \cos \phi_{32} \sin \phi_{31} \\
& + 8C_{13}^2 S_{13}^2 S_{23}^2 \frac{a}{\Delta m_{13}^2} (1 - 2S_{13}^2) \sin^2 \phi_{31}
\end{aligned} \tag{3}$$

where $C_{ij} = \cos \theta_{ij}$, $S_{ij} = \sin \theta_{ij}$ and $\phi_{ji} = \Delta m_{ji}^2 L / 4E_\nu$. The terms that

include a are a consequence of the matter effects with $a = 2\sqrt{2}G_F n_e E_\nu = 7.56 \times 10^{-5} [eV^2] (\rho / (g/cm^3) (E_\nu / GeV)$. The term proportional to $\cos\delta_{CP}$ is invariant for ν and $\bar{\nu}$ whilst the term proportional to $\sin\delta_{CP}$ change if CP is violated. The equivalent term for $P(\bar{\nu}_\mu \rightarrow \bar{\nu}_e)$ can be obtained by reversing the signs of the terms proportional to $\sin\delta_{CP}$ and to a .

These formulas clearly show the complementarity between reactor and long-baseline experiments. The combination of $\bar{\nu}_e$ disappearance from reactors with the measurement of ν_e (and eventually $\bar{\nu}_e$) appearance in long baseline experiments allows to break the degeneracies and access independently to θ_{13} , δ_{CP} and the sign of a .

In this section we will describe the measurements of $\bar{\nu}_e$ disappearance from Daya Bay, RENO and Double Chooz. In addition the combination with measurement of $\bar{\nu}_e$ disappearance provided by The difference between the two channels clearly show the complementarity between reactor and accelerator experiments that can be combined together to measure δ_{CP} and mass hierarchy.

3.5. Measurements of θ_{13} in reactor experiments

reactor flux
 Bugey et al no disappearance
 CHOOZ : theta13 small
 DCHOOZ RENO Daya Bay theta13 prec. measurement ND/FD technique
 bump and uncertainty flux (anomaly) no impact on theta13

3.6. ν_e appearance in long baseline experiments and the quest for δ_{CP}

As mentioned in ??, the main goal of long baseline experiments is nowadays the search for ν_e and $\bar{\nu}_e$ appearance. The ν_e appearance is in fact a sub-leading effect of the disappearance of muon neutrinos depending on a combination of θ_{13} , θ_{23} , δ_{CP} , and mass hierarchy as shown in Eq. ??.

The ν_e appearance phenomenon has been observed for the first time by T2K in 2012 [?]. A total of 28 electron neutrino candidates were detected in Super-Kamiokande while 4.92 ± 0.55 background events were expected for $\theta_{13} = 0$. The $p - \theta$ distribution for these events is shown in Fig ?? and the significance of this measurement correspond to 7.3σ . In 2016 also the NOVA experiment has reported the observation of ν_e appearance, by observing 33 e-like candidates to be compared with an expected background of 8 events (see Fig. ??).

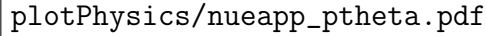


Figure 11: $p - \theta$ (left) and E_ν^{rec} (right) distribution for the ν_e candidates events [?].

By combining the observation of ν_e appearance in long-baseline experiments with the precise measurement of $\bar{\nu}_e$ disappearance with reactors it is possible to extract information on the sub-leading terms entering the appearance probability, particularly the CP violation term δ_{CP} and the mass hierarchy sign. The relative size of the effect on the appearance probability due to δ_{CP} and to the mass ordering depends on the baseline. The effect of the hierarchy is in fact proportional to the amount of matter crossed by neutrinos before reaching the detector.

In the case of T2K the baseline is relatively short (295 km) and the matter effects contribute to $\sim \pm 10\%$ of the oscillation probability while the effect due to δ_{CP} can be as large as $\pm 30\%$ for the extreme values of δ_{CP} as shown in Fig. ???. In the case of NOVA the baseline is 810 km and the effect of the mass ordering and of δ_{CP} on $P(\nu_\mu \rightarrow \nu_e)$ is roughly equal and it corresponds to $\sim 20\%$ for each source.

It is important to notice that for $\bar{\nu}_e$ appearance the signs are reverted. In neutrino mode the appearance probability is maximized for normal hierarchy and $\delta_{CP} = -\pi/2$ while in anti-neutrino mode the appearance probability is maximized for inverted hierarchy and $\delta_{CP} = \pi/2$ as it is shown in Fig. ??

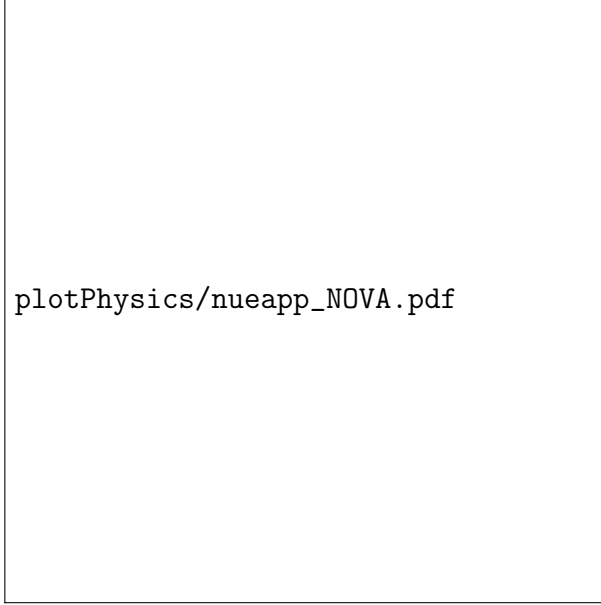


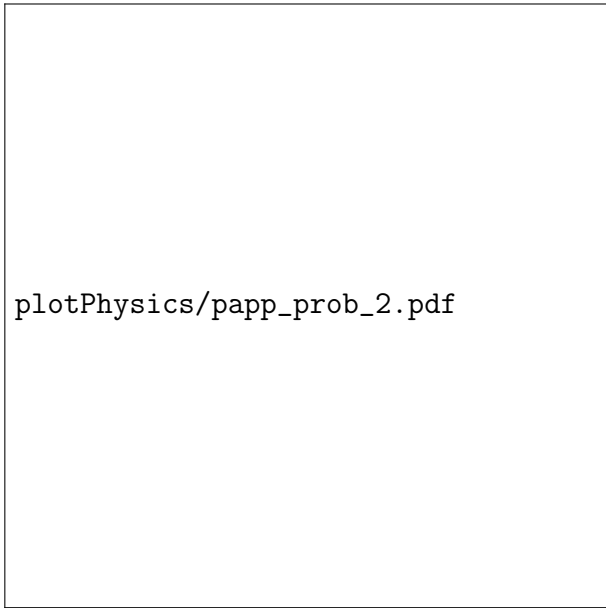
Figure 12: $p - \theta$ (left) and E_ν^{rec} (right) distribution for the ν_e candidates events [?].

for the case of T2K. This figure clearly show the complementarity between $P(\nu_\mu \rightarrow \nu_e)$ and $P(\bar{\nu}_\mu \rightarrow \bar{\nu}_e)$ and illustrates the importance of taking data also focusing anti-neutrino to fully exploit the asymmetry between ν_e and $\bar{\nu}_e$ appearance to measure δ_{CP} .

Finally Eq. ?? shows that the appearance probability also depends on the value of θ_{23} . Long-baseline accelerator experiments searching for ν_e appearance are also sensitive to θ_{23} through ν_μ disappearance. To fully take into account the correlations between oscillation parameters it is preferable to perform a joint analysis of appearance and disappearance. This procedure was used by T2K in [] and for the most recent results presented at Neutrino2016 also the $\bar{\nu}_\mu$ disappearance and the $\bar{\nu}_e$ appearance channels are included into the same fit.

3.6.1. Search for δ_{CP} in T2K and NOVA

In the coming years, before the new projects that will be described in [?] will come online, the quest for the missing parameters in the PMNS scheme (δ_{CP} , mass ordering, θ_{23} octant) will be lead by the two long-baseline accelerator experiments that are currently taking data, namely T2K and NOVA.



plotPhysics/papp_prob_2.pdf

Figure 13: Oscillation probabilities as a function of neutrino energy with $L=295$ km, $\sin^2(2\theta_{13}) = 0.1$, $\delta_{CP} = \pi/2$ and normal hierarchy. The contribution of the different terms of the oscillation probability is shown separately.

The most recent results T2K and NOVA (effect coupled to MH, NOVA if they publish)

nue appearance sensitivity to delta CP (plot)

3.6.2. *Search for δ_{CP} in Super-Kamiokande*

SK effect in atm due to delta

3.7. *PMNS model: summary*

data well described by 3nu oscillations (PMNS)

recent global fit (Concha/FL) table

experiment start to be sensitive to 3nu effects

4. Anomalies (SL)

LSND $\bar{\nu}_\mu \rightarrow \bar{\nu}_e$ → 4th nu

Miniboone inconclusive

reactor anomaly (controversy) - Ga anomaly



Figure 14: Oscillation probabilities as a function of neutrino energy for $P(\nu_\mu \rightarrow \nu_e)$ (left) and $P(\bar{\nu}_\mu \rightarrow \bar{\nu}_e)$ (right) with $L=295$ km and $\sin^2(2\theta_{13}) = 0.1$. The different line colors correspond to different values of δ_{CP} while the solid (dashed) lines represent the normal (inverted) hierarchy.

tension appearance/disappearance (CDHS Daya Bay Bugey)
 3+1 models, bad fits
 need for a clarification exp : test of reactor anomaly reactor(SOLID
 STEREO) + sources (SOX) + accelerators

need to understand the reactor spectrum

5. Perspectives for future experiments 20pg MZ

5.1. Existing projects: T2K NOVA

T2K statx10 + antinu data no MH
NOVA MH sensitivity (depends on delta)
(where do we add SK ?)
increased sensitivity to theta23

5.2. middle term

JUNO prec measurement of theta12 and Dm21
method NH/IH, critics Parke
depends on E exp resolution, not demonstrated
PINGU/ORCA discussion sensitivity MH (numu- $\bar{\nu}$ numu vs showers)
INO distinguishes btw numu and numubar status ?

5.3. Long term: HyperKamiokande, DUNE

DUNE new technology LAr 40 kt new beam
decouples CP violation from MH with nu/nubar beam
HyperK 500 kt fiducial (finance ?) upgraded T2K beam
complementarity DUNE/HK

6. Conclusions

- Aartsen, M., et al., 2016. Neutrino oscillation studies with icecube-deepcore. Nuclear Physics B 908, 161 – 177, neutrino Oscillations: Celebrating the Nobel Prize in Physics 2015.
URL <http://www.sciencedirect.com/science/article/pii/S0550321316300141>
- Abe, K., et al., 2013. Evidence for the Appearance of Atmospheric Tau Neutrinos in Super-Kamiokande. Phys. Rev. Lett. 110 (18), 181802.
- Achar, C. V., et al., 1965. Detection of muons produced by cosmic ray neutrinos deep underground. Phys. Lett. 18, 196–199.
- Agafonova, N., et al., 2015. Discovery of τ Neutrino Appearance in the CNGS Neutrino Beam with the OPERA Experiment. Phys. Rev. Lett. 115 (12), 121802.

- Ahn, M. H., et al., 2006. Measurement of Neutrino Oscillation by the K2K Experiment. *Phys. Rev. D* 74, 072003.
- Barr, G. D., Gaisser, T. K., Lipari, P., Robbins, S., Stanev, T., 2004. A Three - dimensional calculation of atmospheric neutrinos. *Phys. Rev. D* 70, 023006.
- Battistoni, G., Ferrari, A., Montaruli, T., Sala, P. R., 2003. The FLUKA atmospheric neutrino flux calculation. *Astropart. Phys.* 19, 269–290, [Erratum: *Astropart. Phys.* 19, 291(2003)].
- Beavis, D., Carroll, A., Chiang, I., Apr. 1995. Long baseline neutrino oscillation experiment at the AGS. Tech. rep.
- Bernardini, P., Fogli, G., Lisi, E., Crescenzo, A. D., 2015. Proceedings of the neutrino oscillation workshop results from the opera experiment. *Nuclear and Particle Physics Proceedings* 265, 186 – 188.
URL <http://www.sciencedirect.com/science/article/pii/S2405601415003892>
- Fukuda, Y., et al., 1998. Evidence for oscillation of atmospheric neutrinos. *Phys. Rev. Lett.* 81, 1562–1567.
- Gaisser, T. K., Honda, M., 2002. Flux of atmospheric neutrinos. *Ann. Rev. Nucl. Part. Sci.* 52, 153–199.
- Honda, M., Kajita, T., Kasahara, K., Midorikawa, S., Jun 2011. Improvement of low energy atmospheric neutrino flux calculation using the jam nuclear interaction model. *Phys. Rev. D* 83, 123001.
URL <http://link.aps.org/doi/10.1103/PhysRevD.83.123001>
- Hosaka, J., et al., 2006. Three flavor neutrino oscillation analysis of atmospheric neutrinos in Super-Kamiokande. *Phys. Rev. D* 74, 032002.
- Kopp, S. E., 2007. Accelerator neutrino beams. *Physics Reports* 439 (3), 101 – 159.
URL <http://www.sciencedirect.com/science/article/pii/S0370157306004431>
- Reines, F., Crouch, M. F., Jenkins, T. L., Kropp, W. R., Gurr, H. S., Smith, G. R., Sellschop, J. P. F., Meyer, B., 1965. Evidence for high-energy cosmic ray neutrino interactions. *Phys. Rev. Lett.* 15, 429–433.